Removal of Acid Red 131 by Peroxi-Coagulation Using Stainless Steel and Aluminum Electrodes: a Comparative Study

Behnam Nayebi[1] · Mohammad Ghalebizade[1] · Kasra Pourrostami Niavol[1]

Abstract

Azo dyes have great application in industries like textile. However, their presence poses a lot of concerns to the environment and human health such as carcinogenic effect. Electrochemical processes such as peroxi-coagulation (PC) are cost effective and efficient advanced oxidation processes which have been investigated extensively. This study aimed to conduct a comparative study on removal of Acid red 131 as an azo dye via PC process using stainless steel (SS) and aluminum (Al) electrodes as anode and graphite as cathode. Parameters including dye concentration, current density, initial pH, aeration rate, and electrode's surface area were investigated. According to the results, the optimum condition for both electrodes was achieved at electrode's surface area $= 60$ cm^2, pH $= 7$, and aeration rate $= 1.5$ L/min. Also, the optimum current of 0.6 A and 0.9 A were selected for SS and Al, respectively. The removal percentages at these conditions were measured 98% and 93% after 120 min for SS and Al, respectively. Chemical oxygen demand (COD) removal was also investigated, and the removal percentage was recorded 93% and 79% for SS and Al after 180 min, respectively. The removal kinetics studies indicated that the pseudo-first order model best fitted for both electrodes. Based on the results, the SS electrode outperformed the Al electrode and facilitated the process.

Introduction

Industrialization has been identified as the main source of contamination in the environment. Textile, food, leather, pharmaceutical, and paper industries are among the industries with high discharge volume of synthetic dyes through wastewater [1]. It is estimated that approximately 10,000 types of dyes are produced per year around the world [2]. Dyes can be classified mainly into azo, anthraquinone, sulfur, indigo, triphenylmethyl, and phthalocyanine among which azo dyes share 70% of the dye production globally which make them ubiquitous in wastewater streams [3]. Azo dyes have a chromophore group including one or more azo groups (-N = N-) which usually linked with benzene and/or naphthalene systems [4]. Due to their application in industry, azo dyes are stable and resistant to biodegradation, light exposure, and redox reactions [5, 6]. Acid red 131 is

a soluble anionic dye and the sodium salt of sulfonic and carboxylic acids which is used widely in textile industry. However, limited information is available on this dye. The release of this dye into the environment causes esthetic pollution besides toxicity [7].

Common treatments methods such as adsorption are either inefficient or expensive to implement. Therefore, advanced oxidation processes (AOPs) have been investigated for removal of synthetic dyes from wastewater streams. These methods involve chemical [8], photochemical [9], or electrochemical processes in which hydroxyl radicals (OH$^{\bullet}$) production is facilitated [10]. These radicals react with contaminants through hydrogen atom abstraction, electrophilic addition to π systems, and redox reactions [11]. One of the most common AOPs is Fenton-based methods. In Fenton method, H_2O_2 and Fe^{2+} are utilized to eliminate organic compounds through Eq. (1). However, this method needs the supply of H_2O_2 and Fe continuously. Thus, catalytic reactions based on the regeneration of Fe^{2+} ions through Fenton-like reaction (Eq. (2)) have been developed, but the regeneration of Fe^{2+} is extremely slower than Fenton's reaction [12]. Hence, electro-Fenton (EF) technique can be

✉ Kasra Pourrostami Niavol
kasra.pourrostami@gmail.com

1 Civil and Environmental Engineering Faculty, Tarbiat Modares University, P.O. Box 14115-397, Tehran, Iran

used to produce the reagents electrochemically through the process [4].

$$H_2O_2 + Fe^{2+} \rightarrow Fe^{3+} + OH^{\bullet} + OH^- \tag{1}$$

$$H_2O_2 + Fe^{3+} \rightarrow Fe^{2+} + H^+ + OH^- + HO_2^{\bullet} \tag{2}$$
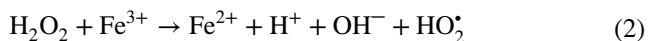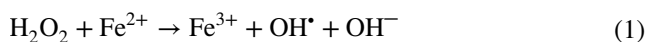
In EF, on the anode surface, hydroxyl radicals can be generated due to water oxidation through Eq. (3). However, it should be noted that the electrogenration hydroxyl radicals depends on the utilization of electrodes with high overpotential of oxygen evolution [13, 14]. In electro-assisted Fenton processes, the regeneration of Fe^{2+} is occurred through electrochemical reduction of Fe^{3+} at the cathode surface Eq. (4) [12, 15]. It is worth mentioning that there are several cathodic materials including carbon nanotubes, activated carbon fiber, graphite felt, carbon felt that can be used to generate H_2O_2 through Eq. (5) [14].

$$H_2O \rightarrow H^+ + OH^{\bullet} + e^- \tag{3}$$

$$Fe^{3+} + e^- \rightarrow Fe^{2+} \tag{4}$$

$$O_2 + 2H^+ + 2e^- \rightarrow H_2O_2 \tag{5}$$

Several parameters affecting the performance of EF process include pH, current, H_2O_2/Fe^{2+} ratio, reaction time, and electrode type [16, 17]. Numerous studies investigated the application of EF process in removal of a wide range of contaminants [18–20]. Can (2019) [21] showed that EF was efficient in decreasing the chemical oxygen demand (COD) of fruit-juice wastewater. In this study, iron and titanium electrodes were used and 10 mL of hydrogen peroxide was added to the process. The results revealed that the 85% of COD in 25 min was removed after EF. Also, different combinations of electrodes have been investigated recently [22, 23]. For example, Yavuz et al. (2014) [24] used one pair of two iron and one aluminum plates as anode and cathode electrodes in EF process. They reported that it could significantly remove Basic Red 29 dye with high efficiency (> 95%).

In addition to EF, electrocoagulation revolves around the separation of contaminants via complexation and sorption mechanisms. Metal anodes like iron and aluminum are used in electrocoagulation to generate metal hydroxides during electrolysis which are responsible for the coagulation process [25]. Recently, peroxi-coagulation (PC) process has been investigated which is the combination of EF and electrocoagulation and is used to treat organic contamination [26]. Thus, PC benefits the synergistic mechanisms of EF and electrocoagulation. In essence, PC comprises of electrogeneration of hydrogen peroxide on cathode surface (Eq. (5) along with coagulation using a sacrificial iron anode to provide ferrous ions (Fe^{2+}) in the solution through

Eq. (6). Afterwards, ferric ions (Fe^{3+}) are reduced at cathode to regenerate ferrous ions in the solution. The redundant Fe^{3+} ions precipitate as $Fe(OH)_3$ through Eq. (7) to enhance the efficiency of the removal process [27, 28].

$$Fe \rightarrow Fe^{2+} + 2e^- \tag{6}$$

$$Fe^{3+} + 3OH^- \rightarrow Fe(OH)_{3\,(s)} \tag{7}$$
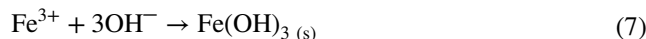
Several studies have been conducted to treat dyes using PC process [29, 30]. However, the studies comparing different electrodes including aluminum for PC process are rare. Moreover, although electrochemical processes have been used widely to treat dye pollution, few studies on the removal dyes using PC system have been published [31]. Additionally, Thus, this increases the need to investigate the removal of this dye using different processes [7]. This study aimed to conduct a comparative study to investigate the effects of different parameters including pH, electrode surface area, dye concentration, current, and aeration rate on the removal of Acid red 131 dye using stainless steel and aluminum electrodes during PC process. In addition, kinetic studies for the two electrodes were conducted to provide an overview of the removal kinetics. The results of this study can be used as a tool to compare the performance of stainless steel and aluminum electrodes and provides an overview of affecting parameters on the PC process.

Materials and Methods

Materials

To provide conductivity in the experimental cell, Na_2SO_4 (Merck) was used as electrolyte. Acid red 131 ($C_{30}H_{21}N_3NaO_9S_2$) was purchase locally and used to prepare stock solutions. The structure of the dye is shown in Fig. 1.
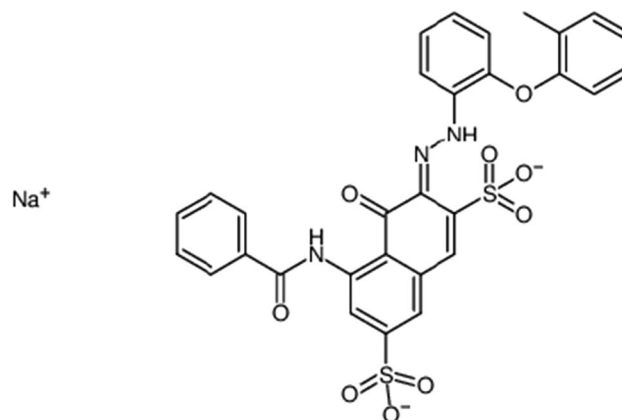

Fig. 1 The chemical structure of Acid red 131

Table 1 Characteristics of acid red 131

Parameter	Value
Chemical class	Monoazo
Odor	Odorless
Dye group	Anionic
Solubility in water (g/L)	100
Acute toxicity (g/kg)	> 5
λ_{max} (nm)	548

Table 2 Parameter's initial values

Parameter	Initial value
pH	3, 7, 9
Electrode surface (cm^2)	15, 30, 60
Current (A)	0.3, 0.6, 0.9, 1.2
Aeration flow (L/min)	0, 1.5, 3
Initial dye concentration (mg/L)	35, 50,100, 150

Also, the characteristics of Acid red 131 are presented in Table 1. To adjust pH of the solution, H_2SO_4 and NaOH (Merck, Germany) were used. It is worth mentioning that all chemicals used in this study were analytical grades. Rectangular stainless steel 304 plate, aluminum plate, and graphite cathode with length of 15 cm, depth of 6 mm and variable width were purchased locally for the electrode materials.

Experimental Setup

Experimental tests were conducted in an electrochemical cell made of Plexiglas with a working volume of 500 ml. Stainless steel (SS) and aluminum (Al) were selected as anode electrodes while the cathode was made of graphite and was placed at a 3 cm distance from the anode. Additionally, air was injected close to the cathode using an air pump (Danner-AP4) in order to increase the soluble oxygen in the solution to enhance hydrogen peroxide generation. Also, the air flow was controlled by a flowmeter (Dwyer, VFA-23). Regarding homogenization, the solution was mixed at 1000 rpm using a magnetic stirrer (Intllab- MS-500). The power was generated by a power supply (Instek-GPS1850D). Initial pH of solutions was measured using a handheld pH meter (Oakton, pH 5 +).

Experimental Procedure

A stock solution of Acid red 131 with 1000 mg/L concentration was prepared and then favorable concentrations were made from the stock solution. Na_2SO_4 was added to the solution to reach the concentration of 0.01 M to provide electrolyte for the ionic strength of the solution. It should be noted that as mentioned above, peroxi-coagulation works on iron anode. However, in this study another type of anode was tested in PC process. Therefore, to provide iron content in Al anode tests, iron (Fe^{2+}) with concentration of 0.5 mM was added to the solution. In this study, changes in main parameters including initial dye concentration, current, pH, aeration flow, electrode surface, and COD were investigated. COD was measured according to the standard method for water and wastewater examination [32]. The initial values for each parameter are shown in Table 2. Samples were taken every

30 min from the solution to measure the concentration of the dye using a spectrophotometer (Hach-DR5000) at 548 nm wavelength. The decolorization percentage of the dye was calculated using Eq. (8) [33]. Furthermore, the kinetics of Acid red 131 removal were analyzed using pseudo first and second order reaction kinetics [34].

$$R(\%) = \frac{A_0 - A_F}{A_0} \times 100 \tag{8}$$

where, R (%) is the decolorization percentage of the dye. A_0 and A_F are the initial and final absorbance at 548 nm after the retention time, respectively.

Energy Consumption

The performance of SS and Al electrodes were also compared in terms of energy consumption (EC) calculated with the modified Eq. (9) [19].

$$EC = \frac{V \times I \times t \times 1000}{M \times V_c} \tag{9}$$

where EC is energy consumption (KWh/kg), V is voltage (V), I is current (A), t is time (hr), M is the concentration of the dye removed in the process (mg/L), and V_c is the cell's volume (L).

Results and Discussion

Effect of Initial Dye Concentration

Initial dye concentration is an important parameter in electrochemical processes since it can provide an overview of the concentration range in which the pollutant of interest can be removed efficiently. The effect of different initial dye concentrations on the performance of the system using different electrodes was investigated and the results are shown in Fig. 2a-b. Results showed that the dye was removed efficiently (> 90%) in 120 min when the concentration was lower than 100 mg/L. Additionally, as the dye concentration rose above 100 mg/L, the dye concentration decreased slowly, and more retention time was required to accomplish
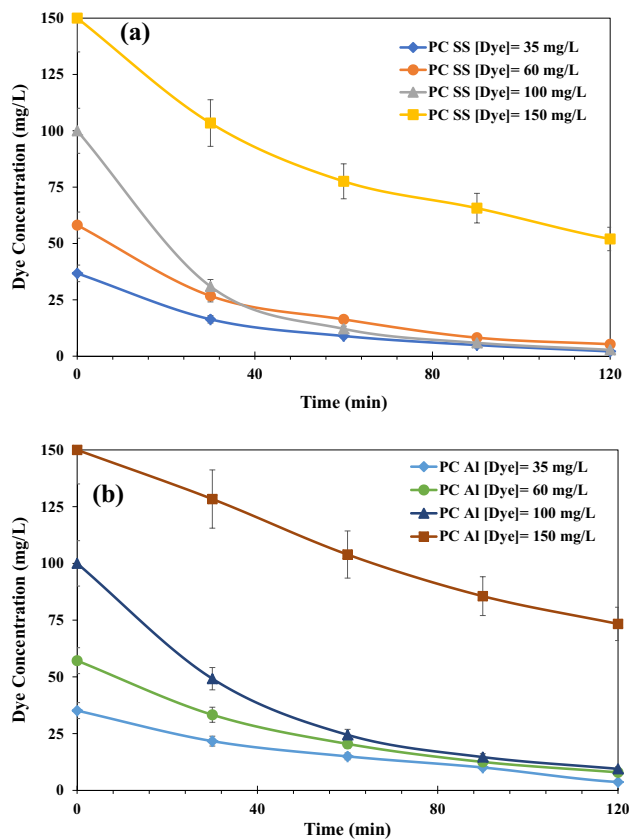
Fig. 2 **a** The performance SS system based on different initial dye concentrations. (A = 0.9 A, pH = 7, air flow = 1.5 L/min, electrode surface = 60 cm^2). **b** The performance Al system based on different initial dye concentrations. (A = 0.9 A, pH = 7, air flow = 1.5 L/min, electrode surface = 60 cm^2)

Fig. 3 The energy consumption of Al and SS systems at different initial dye concentrations. (A = 0.9 A, pH = 7, air flow = 1.5 L/min, electrode surface = 60 cm^2)

In addition, EC of the electrodes towards different initial dye concentration was investigated which is illustrated in Fig. 3. Based on the results, EC for the concentration range of 35–100 mg/L decreased as concentration increased. On the other hand, when concentration exceeded 100 mg/L, EC increased accordingly. According to Fig. 3, the optimum concentration for both electrodes was 100 mg/L which resulted in values of 0.21 and 0.34 KWh/kg for SS and Al, respectively. This trend can be interpreted as the oxidants concentration in the solution was constant, so increasing the amount of dye could facilitate the interactions between dye and oxidants which gave rise to efficient energy consumption [6].

Effect of Applied Current

As mentioned in Eqs. (1) and (3), the degradation of pollutants is dependent on OH$^\bullet$ and H$_2$O$_2$ generation. H$_2$O$_2$ is usually produced by oxygen reduction on the surface of a carbon-based electrode like graphite. In the present study, hydrogen peroxide was produced continuously using constant aeration close to a graphite electrode. It has been reported that H$_2$O$_2$ production rate is directly related to the amount of current applied in the system [38, 39]. In this regard, the effect of current was investigated with different values (0.3, 0.6, 0.9, and 1.2 A) for SS and Al anodes.

Figure 4a–b shows that as the current increased, the decolorization of Acid red 131 enhanced proportionally so that it was improved from 70 to 94% and 85 to 98% after 120 min for Al and SS, respectively. This phenomenon is probably because of faster and higher generation of H$_2$O$_2$, OH$^\bullet$ radicals, and Fe(OH)$_3$ flocs as the current increased [40]. Moreover, higher currents could lead to faster generation of Fe^{2+} which accelerated the generation of oxidizing agents [41, 42]. In addition to oxidation, coagulation plays an important role in PC systems. Thus, as the current density

more than 90% removal. The final dye concentrations at 150 mg/L after 120 min were recorded 73 and 52 mg/L for Al and SS, respectively. This decrease in the decolorization percentage of higher concentrations might be attributed to the higher requirement of oxidizing agents at higher concentrations whereas the generation rate of hydroxyl radicals was constant in the system because other parameters were constant. Therefore, the decolorization percentage decreased [35]. Additionally, when all other parameters, expect for initial concentration, were constant the amount of coagulants produced during PC, is limited. Therefore, at high concentrations, like oxidizing agents, sufficient coagulants are not present in the solution [36].

The results obtained were in accordance with previous published studies. Results published by Salari et al. (2009) [37] revealed that decreasing the Basic Yellow 2 gave rise to rapid removal of the dye concentration in PC process. Similarly, Ren et al. (2018) [26] showed when the initial concentration of acrylonitrile increased from 50 to 500 mg/L, the removal efficiency decreased from 94 to 80% using modified graphite felt cathode in PC process.
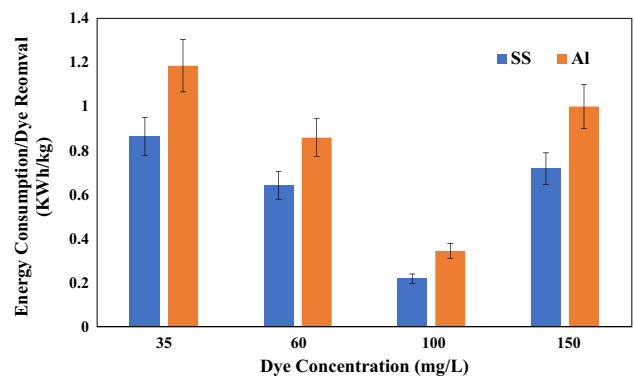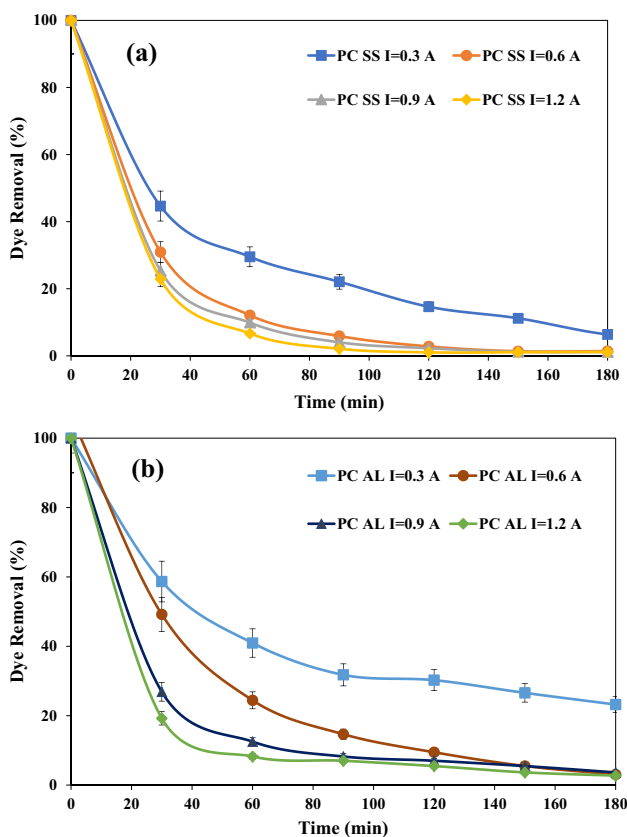
Fig. 4 **a** The effect of current on the performance of SS system. (Dye concentration = 100 mg/L, pH = 7, Air flow = 1.5 L/min, Electrode surface = 60 cm²). **b** The effect of current on the performance of Al system. (Dye concentration = 100 mg/L, pH = 7, Air flow = 1.5 L/min, Electrode surface = 60 cm²)

Fig. 5 The energy consumption of Al and SS systems for the removal percentage of 95% at different currents. (Dye concentration = 100 mg/L, pH = 7, Air flow = 1.5 L/min, Electrode surface = 60 cm²)

increased in the system the $Fe(OH)_3$ and $Al(OH)_3$ flocs increased [43]. Also, higher density could lead to smaller bubbles which in turn increased the removal by flotation [44]. In a study, Ren et al. (2018) [26] revealed that increasing current intensity from 50 to 300 mA could enhance the removal efficiency of acrylonitrile by 20%. Based on the abovementioned reasons, the SS electrode outperformed Al as it released more iron ions to the solution along with faster peroxide generation and $Fe(OH)_3$ flocs.

Furthermore, as shown in Fig. 4a–b, the decolorization efficiency did not change dramatically at currents higher than 0.6 and 0.9 A for SS and Al, respectively. This can be attributed to two reasons. First, increasing current may have led to decreasing flocs size dramatically that impeded the efficiency of coagulation process in both systems [43]. Second, the increased Fenton reagents in the SS system and wasting of hydroxyl radicals through the Eqs. (10) to (12) might have happened [45]. Additionally, in the Al system, since there were no excess iron ions, increasing current higher than 0.9 A, did not enhance the oxidation process and electrocoagulation dominated which released excess aluminum ions and
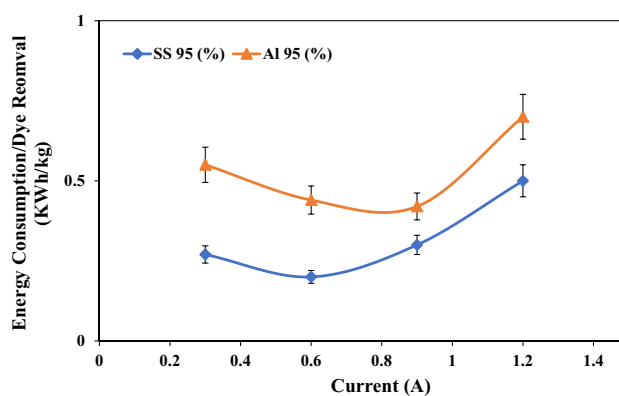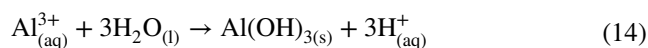
$Al(OH)_3$ via Eqs. (13) and (14) that could have impeded the coagulation process [46, 47]. According to the results, it can be inferred that the iron content added in the Al system was not sufficient to provide oxidation process, and further studies are recommended on finding the optimum Fe concentration in Al systems.

$$Fe^{2+} + OH^\bullet \rightarrow Fe^{3+} + OH^- \tag{10}$$

$$H_2O_2 + OH^\bullet \rightarrow HO_2^\bullet + H_2O \tag{11}$$

$$OH^\bullet \rightarrow O_{2(g)} + 2H^+ + 2e^- \tag{12}$$

$$Al_{(s)} \rightarrow Al^{3+}_{(aq)} + 3e^- \tag{13}$$

$$Al^{3+}_{(aq)} + 3H_2O_{(l)} \rightarrow Al(OH)_{3(s)} + 3H^+_{(aq)} \tag{14}$$

In this regard, the currents of 0.9 A and 0.6 A were selected as the optimum values for Al and SS in the following experiments, respectively. Figure 5 shows EC for the two electrodes reaching 95% decolorization percentage. The EC for Al electrode was calculated 0.42 KWh/Kg for the selected removal percentage at the optimum current. On the other hand, the EC value when SS electrode was used was obtained 0.2 KWh/Kg for 95% removal percentage at the optimal current.

Effect of Initial pH

Solution pH plays critical role in electrochemical processes since it controls the generation of free radicals and ferrous ions [48]. Three different pH values indicating acidic (pH = 3), neutral (pH = 7) and basic (pH = 9)

condition were selected to investigate the effect of initial pH. Figure 6a–b shows that as the pH increased from acidic to basic, the decolorization efficiency decreased. In acidic condition, the removal efficiency after 60 min of the reaction was achieved 90% and 83% for SS and Al, respectively. Fe^{2+} and H^+ are the main two ions that are important in PC process. As mentioned above, H^+ can facilitate the generation of H_2O_2 in the solution via Eq. (5), but H^+ can also act as an electron scavenger in highly acidic pH via Eq. (15) [49]. In contrast, at alkaline pH the Fe^{3+} precipitates in the form of $Fe(OH)_3$ and $FeOOH^{2+}$ in SS system which diminishes the efficacy of the process and replace the process with coagulation [50, 51]. On the other hand, in the Al system, mainly $Al(OH)_3$ produced which had lower efficiency than $Fe(OH)_3$ [44]. At neutral pH, the decolorization efficiency compared to acidic pH slightly decreased and the dye removal percentage was measured 87% and 79% for SS and Al, respectively. At this pH, since $Fe(OH)_3$ flocs formed, the removal mechanisms can be attributed to complexation or electrostatic attraction [52].

This shows that the main removal mechanism in PC with both electrodes could be attributed to coagulation rather than oxidation because the removal efficiency did not differ from one another at acidic and neutral pH [53]. However, in the SS system, higher removal could be attributed to the help of oxidation to the coagulation process. Also, since reaching acidic pH needs chemical consumption and the difference was negligible, the pH of 7 was selected as the optimal value for further experiments.

$$OH^\bullet + H^+ + e^- \rightarrow H_2O \qquad (15)$$

do Vale-Júnior et al. (2018) [30] studied the treatment of Methyl Orange dye using PC treatment method. They reported that when the pH increased from 3 to 7, the removal efficiency decreased since hydroxyl radicals were not generated at higher pH. In another study, Venu et al. (2016) [52] revealed that when the solution pH increased from 3, electro-coagulation mechanism dominated in PC process. Based on the previous studies, coagulation was found to be dominant in the removal process rather than degradation in this study.
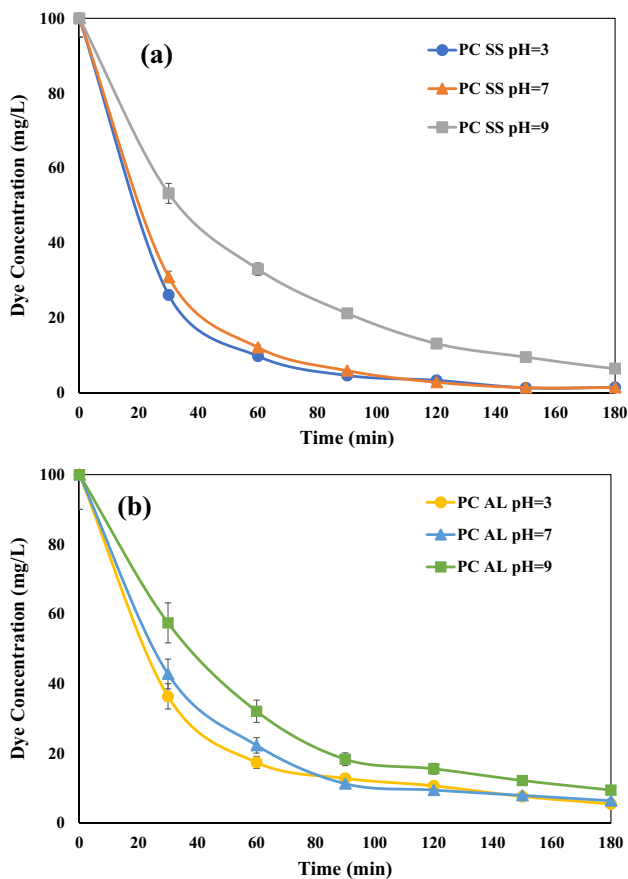
Effect of Aeration Rate

In this step, air was injected continuously during the process to increase the dissolved oxygen's level in the solution near the graphite cathode. Thus, H_2O_2 could be produced via Eq. (5) on the cathode surface. In PC process, presence of H_2O_2 is of importance since it can give rise to free radicals' generation as mentioned in Eq. (1). To investigate the effect of aeration rate, three different rates were determined. Figure 7a illustrates that for SS anode the decolorization percentage after 60 min increased by 17% when the air flow increased up to 1.5 L/min. However, if the air flow increased to 3 L/min the decolorization percentage slightly decreased after 60 min. This can be interpreted as at high air flow hydrogen peroxide reacted as radical scavenger as mentioned in Eq. (11). On the other hand, as shown in Fig. 7b, increasing the aeration percentage caused 12% enhancement in the decolorization percentage when the aeration rate was increased from 0 to 1.5 L/min for Al electrode. However, when the aeration rate increased to 3 L/min the removal percentage decreased by 10% probably because in Al system when the peroxide concentration increased in the system, the scavenging effect of excess H_2O_2 highly affected the system in comparison to SS system. Additionally, another reason that the efficiency reduced in both systems was possibly due to the fact that increasing the air flow, increases the bubbles around the electrode and consequently decreases the efficiency of H_2O_2 production and flocs formation [54]. Therefore, the aeration rate of 1.5 L/min was selected as the optimum value for SS and Al anodes.
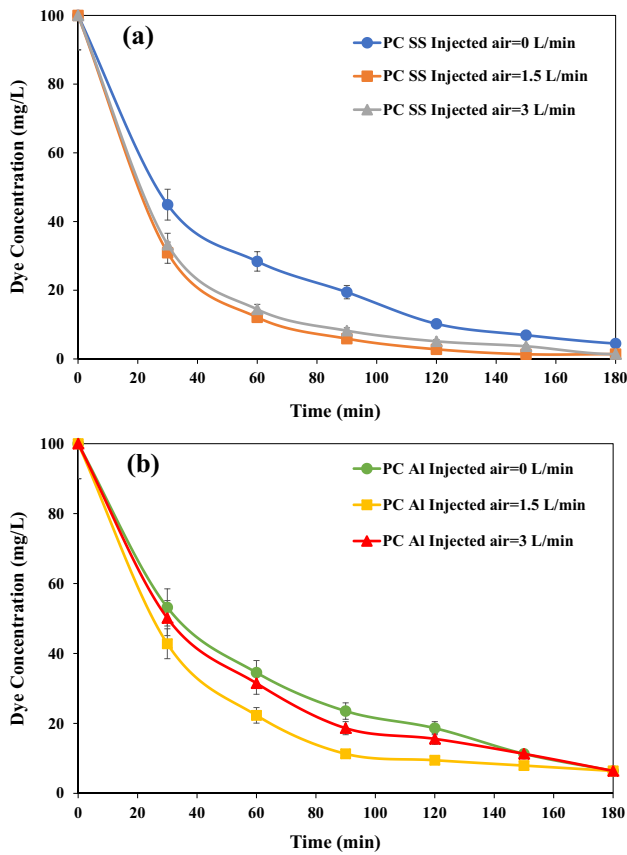

Fig. 6 a The effect of initial pH on the performance of SS system. (Dye concentration = 100 mg/L, Current = 0.6 A, Air flow = 1.5 L/min, Electrode surface = 60 cm^2). **b** The effect of initial pH on the performance of Al system. (Dye concentration = 100 mg/L, Current = 0.9 A, Air flow = 1.5 L/min, Electrode surface = 60 cm^2)

Fig. 7 **a** The effect of air injection rate on the performance of SS system. (Dye concentration = 100 mg/L, Current = 0.6 A, pH = 7, Electrode surface = 60 cm^2). **b** The effect of air injection rate on the performance of Al system. (Dye concentration = 100 mg/L, Current = 0.9 A, pH = 7, Electrode surface = 60 cm^2)

Effect of Electrode's Surface Area

The electrode's surface area is another main parameter affecting the PC process since it can accelerate the degradation kinetics and H$_2$O$_2$ generation [55]. To investigate the effect of electrode's surface, three different areas (15, 30, 60 cm^2) were studied. Figure 8a–b shows that when the electrode's surface increased, the decolorization percentage enhanced. The removal percentage when the area increased from 15 to 60 cm^2, increased 20% and 17% for Al and SS electrodes after 60 min, respectively. Higher efficiency of larger electrode surface can be interpreted as more bubbles were produced in larger surface leading to better formation of Al(OH)$_3$ and Fe(OH)$_3$ flocs. Also, bigger electrodes could cause more oxidants generation in the process.

Additionally, Fig. 9 presents EC for different electrode sizes to achieve 95% decolorization percentage. According to the results, for the SS electrode, as the surface increased, the EC slightly increased. The EC values were measured 0.13, 0.16, and 0.18 KWh/kg of the dye
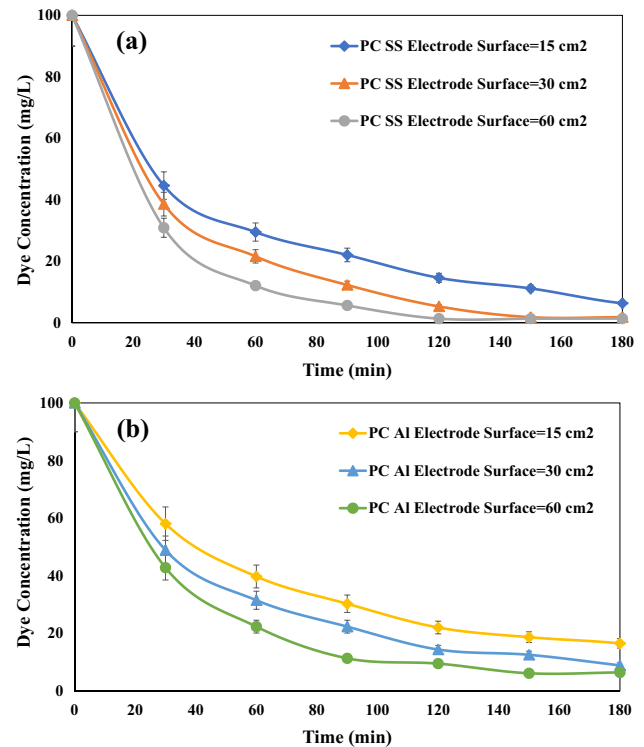
Fig. 8 **a** The effect of electrode surface on the performance of SS system. (Dye concentration = 100 mg/L, Current = 0.6 A, Air flow = 1.5 L/min, pH = 7). **a** The effect of electrode surface on the performance of Al system. (Dye concentration = 100 mg/L, Current = 0.9 A, Air flow = 1.5 L/min, pH = 7)

consumed for 15, 30, and 60 cm^2, respectively. Similarly, for the Al electrode, the EC increased as the size became bigger. The EC values for Al electrode were measured 0.2, 0.32, and 0.44 KWh/kg of the dye removed for 15, 30, and 60 cm^2.
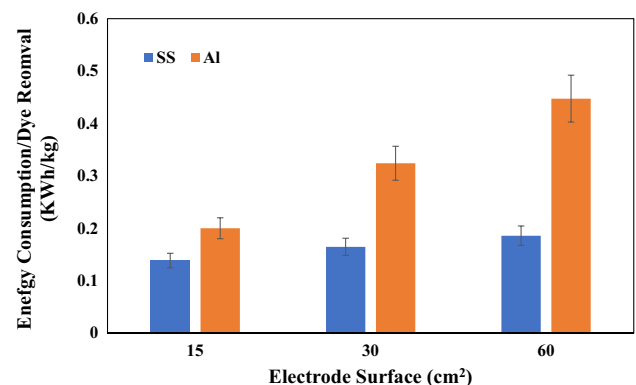

Fig. 9 The energy consumption of the electro-Fenton systems based on electrode surface. (Dye concentration = 100 mg/L, Current = 0.6 (SS) and 0.9 (Al) A, Air flow = 1.5 L/min, pH = 7)

COD Removal

The systems' performance was assessed with respect to COD removal (shown in Fig. 10) when all parameters were optimized. According to the results, the final COD removal was achieved 93% and 79% after 180 min for SS and Al, respectively. As it is shown, the removal percentage was higher at the beginning whereas the slope was weakened as the process continued. This can be due to the cleavage of aromatic rings and transformation to aliphatic compounds which have lower reactivity to OH radicals [56]. With respect to the results obtained in this study, it can be inferred that the amount of iron added to Al system was not enough to provide oxidation in the system, while SS system benefited from coagulation and oxidation simultaneously. The results from Nayir et al. (2020) [57] showed that at the optimum condition (pH = 7 and current = 45 mA/cm^2), 75% of laundry wastewater COD could be removed after 30 min of PC process.

Kinetics Studies

The kinetics of Acid red 131 removal were investigated using the pseudo-first (Fig. 11a and second order (Fig. 11b equations at optimum condition. According to Table 3, the removal kinetics completely fitted with both equations while the pseudo-first order reaction had higher R^2 (0.99 and 0.97 for SS and Al anodes, respectively). Therefore, it was selected as the best model defining the removal kinetics. The higher apparent rate constants for SS show that the removal process was faster when SS electrode was used. Brillas et al. (2003) [58] studied PC and photoperoxi-coagulation (PPC) in removal of 4-chlorophenoxyacetic acid. They reported pseudo first-order rate constant of 0.2 min^{-1} and 0.14 min^{-1} for PPC and PC, respectively. In another study, Sandhwar and Prasad (2018) [59] investigated the

Fig. 11 **a** Pseudo first-order reaction model for both systems at their optimum condition. **b** Pseudo second-order reaction model for both systems at their optimum condition

degradation kinetics of terephthalic acid wastewater using electrocoagulation, peroxi-coagulation, and peroxi-electro-coagulation. They reported that peroxi-electrocoagulation had the highest first order rate followed by peroxi-coagulation and electrocoagulation.

Conclusion

A comparative study was performed in order to investigate the performance of SS and Al electrodes in the decolorization of Acid red 131 by PC process. It was observed that parameters such as applied current, initial pH, aeration flow rate, and electrode's surface area had crucial effect on the performance. The reaction kinetics for both electrodes followed pseudo-first order model ($R^2 > 94\%$). The optimum
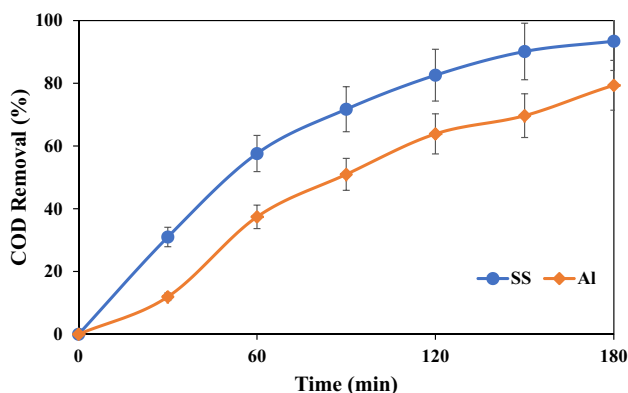

Fig. 10 The COD removal efficiency of the two electro-Fenton systems. (Dye concentration = 100 mg/L, Current = 0.6 (SS) and 0.9 (Al) A, Air flow = 1.5 L/min, Electrode surface = 60 cm^2, pH = 7)
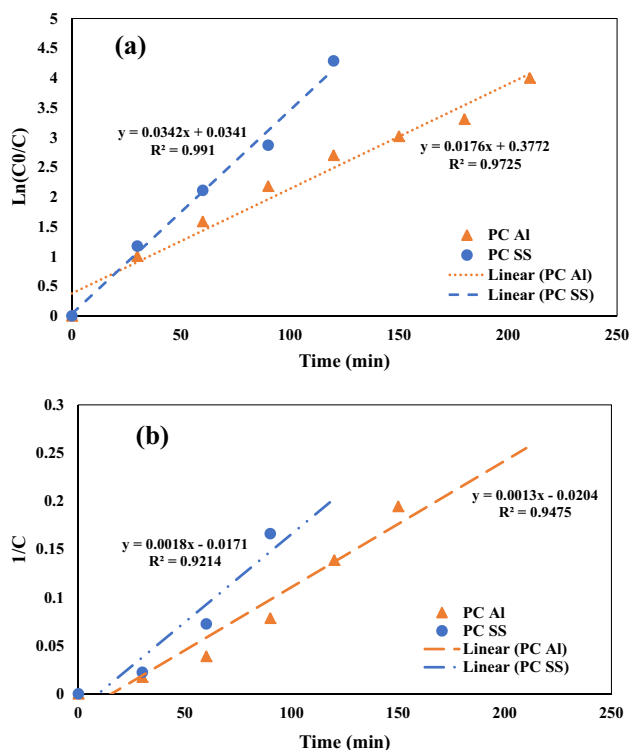
Table 3 Removal kinetics parameters at optimum condition for SS an Al electrode

Electrode	Pseudo-first order		Pseudo-second order	
	R^2	k_1 (min^{-1})	R^2	k_2 (L/mg.min)
SS	0.99	0.0342	0.92	0.0018
Al	0.97	0.0176	0.94	0.0013

condition for both electrodes was found at neutral pH, current of 0.6 A for SS and 0.9 A for Al, air flow of 1.5 L/min and electrode's size of 60 cm^2. Furthermore, both systems were capable of COD removal more than 80% after 180 min. Based on the results, SS electrode outperformed Al, mainly due to the constant supply of iron in the solution. Also, it seemed that coagulation dominated when Al electrode was used while at SS electrode, a combination of coagulation and oxidation was occurred. For future studies, it is recommended investigate different concentrations of iron for addition in Al system. Also, to study the main mechanism governing the removal in both systems, it is recommended to assess the generation of H_2O_2 and analyzed the produced sludge.

Declarations

References

1. Rahmati R, Nayebi B, Ayati B (2021) Investigating the effect of hydrogen peroxide as an electron acceptor in increasing the capability of slurry photocatalytic process in dye removal. Water Sci Technol. https://doi.org/10.2166/wst.2021.136

2. Ferrero F, Periolatto M (2012) Functionalized fibrous materials for the removal of dyes. Clean Technol Environ Policy 14:487–494. https://doi.org/10.1007/s10098-011-0442-5

3. J Perera Ã (2019) Removal of acid orange 7 dye from wastewater: review. Int J Waste Resour 09. https://doi.org/10.35248/2252-5211.19.9.367

4. Brillas E, Garcia-Segura S (2016) Solar photoelectro-fenton degradation of acid orange 7 azo dye in a solar flow plant: optimization by response surface methodology. Water Conserv Sci Eng 1:83–94. https://doi.org/10.1007/s41101-016-0005-z

5. Forgacs E, Cserháti T, Oros G (2004) Removal of synthetic dyes from wastewaters: a review. Environ Int 30:953–971. https://doi.org/10.1016/j.envint.2004.02.001

6. Ghalebizade M, Ayati B (2019) Acid Orange 7 treatment and fate by electro-peroxone process using novel electrode arrangement. Chemosphere 235:1007–1014. https://doi.org/10.1016/j.chemosphere.2019.06.211

7. Khandegar V, AnilK S (2014) Electrochemical treatment of textile effluent containing acid red 131 dye. J Hazard Toxic Radioact Waste 18:38–44. https://doi.org/10.1061/(asce)hz.2153-5515.0000194

8. Fernandes NC, Brito LB, Costa GG et al (2018) Removal of azo dye using Fenton and Fenton-like processes: evaluation of process factors by Box-Behnken design and ecotoxicity tests. Chem Biol Interact 291:47–54. https://doi.org/10.1016/J.CBI.2018.06.003

9. Bahadori E, Rapf M, di Michele A, Rossetti I (2020) Photochemical vs. photocatalytic azo-dye removal in a pilot free-surface reactor: is the catalyst effective? Sep Purif Technol 237:116320. https://doi.org/10.1016/J.SEPPUR.2019.116320

10. Le Huong TX, Alemán B, Vilatela JJ et al (2018) Enhanced electro-fenton mineralization of acid orange 7 using a carbon nanotube fiber-based cathode. Front Mater 5. https://doi.org/10.3389/fmats.2018.00009

11. dos Santos AJ, Fajardo AS, Kronka MS et al (2021) Effect of electrochemically-driven technologies on the treatment of endocrine disruptors in synthetic and real urban wastewater. Electrochim Acta 376:138034. https://doi.org/10.1016/J.ELECTACTA.2021.138034

12. de Luna MDG, Gumaling RP, Barte EG et al (2021) Electrochemically-driven regeneration of iron (II) enhances Fenton abatement of pesticide cartap. J Hazard Mater 126713. https://doi.org/10.1016/J.JHAZMAT.2021.126713

13. Panizza M, Cerisola G (2009) Direct And Mediated Anodic Oxidation of Organic Pollutants. Chem Rev 109:6541–6569. https://doi.org/10.1021/cr9001319

14. Garcia-Segura S, Lima ÁS, Cavalcanti EB, Brillas E (2016) Anodic oxidation, electro-Fenton and photoelectro-Fenton degradations of pyridinium- and imidazolium-based ionic liquids in waters using a BDD/air-diffusion cell. Electrochim Acta 198:268–279. https://doi.org/10.1016/J.ELECTACTA.2016.03.057

15. Davarnejad R, Sabzehei M, Parvizi F et al (2019) Study on soybean oil plant wastewater treatment using the electro-fenton technique. Chem Eng Technol 42:2717–2725. https://doi.org/10.1002/ceat.201800765

16. Mohajeri S, Hamidi AA, Isa MH, Zahed MA (2019) Landfill leachate treatment through electro-fenton oxidation. Pollution 5:199–209. https://doi.org/10.22059/poll.2018.249210.364

17. Dehboudeh M, Dehghan P, Azari A, Abbasi M (2020) Experimental investigation of petrochemical industrial wastewater treatment by a combination of integrated fixed-film activated sludge (IFAS) and electro-Fenton methods. J Environ Chem Eng 8. https://doi.org/10.1016/j.jece.2020.104537

18. Nidheesh PV, Gandhimathi R (2012) Trends in electro-Fenton process for water and wastewater treatment: an overview. Desalination 299:1–15. https://doi.org/10.1016/j.desal.2012.05.011

19. Huo S, Necas D, Zhu F et al (2021) Anaerobic digestion wastewater decolorization by H2O2-enhanced electro-Fenton coagulation following nutrients recovery via acid tolerant and protein-rich Chlorella production. Chem Eng J 406. https://doi.org/10.1016/j.cej.2020.127160

20. Chu Y, Miao B, Zhang X, Lv R (2020) Heterogeneous electro-Fenton-like oxidation for the degradation of 4-nitrophenol characterized by immobilized Fe(III): performance, mechanism and chlorinated organic compounds formation. J Water Process Eng 38. https://doi.org/10.1016/j.jwpe.2020.101662

21. Can OT (2014) COD removal from fruit-juice production wastewater by electrooxidation electrocoagulation and electro-Fenton processes. Desalin Water Treat 52:65–73. https://doi.org/10.1080/19443994.2013.781545

22. Brillas E, Martínez-Huitle CA (2015) Decontamination of wastewaters containing synthetic organic dyes by electrochemical methods. An updated review. Appl Catal B 166–167:603–643. https://doi.org/10.1016/j.apcatb.2014.11.016

23. Adimi M, Mohammad Mohebizadeh S, Poor MM et al (2019) Treatment of Shazand Petrochemical Co., Effluent using electro-fenton method modified with iron nanoparticles and anodic

aluminum oxide electrode: a comparison. Iran J Sci Technol Trans A Sci 43:2799–2806. https://doi.org/10.1007/s40995-019-00766-6

24. Yavuz Y, Shahbazi R, Koparal AS, Öğütveren ÜB (2014) Treatment of Basic Red 29 dye solution using iron-aluminum electrode pairs by electrocoagulation and electro-Fenton methods. Environ Sci Pollut Res 21:8603–8609. https://doi.org/10.1007/s11356-014-2789-8

25. Nidheesh, PV (2018) Removal of organic pollutants by peroxicoagulation. Environ Chem Lett 16:1283–1292. https://doi.org/10.1007/s10311-018-0752-5

26. Ren G, Zhou M, Su P et al (2018) Highly energy-efficient removal of acrylonitrile by peroxi-coagulation with modified graphite felt cathode: Influence factors, possible mechanism. Chem Eng J 343:467–476. https://doi.org/10.1016/J.CEJ.2018.02.115

27. Garcia-Segura S, Eiband MMSG, de Melo JV, Martínez-Huitle CA (2017) Electrocoagulation and advanced electrocoagulation processes: a general review about the fundamentals, emerging applications and its association with other technologies. J Electroanal Chem 801:267–299

28. Brillas E, Casado J (2002) Aniline degradation by Electro-Fenton® and peroxi-coagulation processes using a flow reactor for wastewater treatment. Chemosphere 47:241–248. https://doi.org/10.1016/S0045-6535(01)00221-1

29. Zarei M, Salari D, Niaei A, Khataee A (2009) Peroxi-coagulation degradation of C.I. Basic Yellow 2 based on carbon-PTFE and carbon nanotube-PTFE electrodes as cathode. Electrochim Acta 54:6651–6660. https://doi.org/10.1016/j.electacta.2009.06.060

30. do Vale-Júnior E, da Silva DR, Fajardo AS, Martínez-Huitle CA (2018) Treatment of an azo dye effluent by peroxi-coagulation and its comparison to traditional electrochemical advanced processes. Chemosphere 204:548–555. https://doi.org/10.1016/j.chemosphere.2018.04.007

31. Nidheesh PV, Zhou M, Oturan MA (2018) An overview on the removal of synthetic dyes from water by electrochemical advanced oxidation processes. Chemosphere 197:210–227. https://doi.org/10.1016/J.CHEMOSPHERE.2017.12.195

32. Association APH, Association AWW, Federation WE (2017) Standard methods for the examination of water and wastewater. American Public Health Association

33. Phetrak A, Westerhoff P, Garcia-Segura S (2020) Low energy electrochemical oxidation efficiently oxidizes a common textile dye used in Thailand. J Electroanal Chem 871:114301. https://doi.org/10.1016/J.JELECHEM.2020.114301

34. Stupar SL, Grgur BN, Radišić MM et al (2020) Oxidative degradation of Acid Blue 111 by electro-assisted Fenton process. J Water Process Eng 36. https://doi.org/10.1016/j.jwpe.2020.101394

35. Zarei M, Niaei A, Salari D, Khataee AR (2010) Removal of four dyes from aqueous medium by the peroxi-coagulation method using carbon nanotube–PTFE cathode and neural network modeling. J Electroanal Chem 639:167–174. https://doi.org/10.1016/J.JELECHEM.2009.12.005

36. Palanisamy S, Nachimuthu P, Awasthi MK et al (2020) Application of electrochemical treatment for the removal of triazine dye using aluminium electrodes. J Water Supply Res Technol AQUA 69:345–354. https://doi.org/10.2166/aqua.2020.109

37. Salari D, Niaei A, Khataee A, Zarei M (2009) Electrochemical treatment of dye solution containing CI Basic Yellow 2 by the peroxi-coagulation method and modeling of experimental results by artificial neural networks. J Electroanal Chem 629:117–125

38. Brillas E, Sauleda R, Casado J (1998) Degradation of 4-chlorophenol by anodic oxidation, electro-fenton, photoelectro-fenton, and peroxi-coagulation processes. J Electrochem Soc 145:759–765. https://doi.org/10.1149/1.1838342

39. Boye B, Dieng MM, Brillas E (2003) Electrochemical degradation of 2,4,5-trichlorophenoxyacetic acid in aqueous medium by peroxi-coagulation. Effect of pH and UV light. Electrochim Acta 48:781–790. https://doi.org/10.1016/S0013-4686(02)00747-8

40. Ghanbari F, Moradi M (2015) A comparative study of electrocoagulation, electrochemical Fenton, electro-Fenton and peroxicoagulation for decolorization of real textile wastewater: electrical energy consumption and biodegradability improvement. J Environ Chem Eng 3:499–506. https://doi.org/10.1016/j.jece.2014.12.018

41. Martínez-Huitle CA, Brillas E (2009) Decontamination of wastewaters containing synthetic organic dyes by electrochemical methods: a general review. Appl Catal B 87:105–145. https://doi.org/10.1016/j.apcatb.2008.09.017

42. Khataee AR, Safarpour M, Zarei M, Aber S (2011) Electrochemical generation of H_2O_2 using immobilized carbon nanotubes on graphite electrode fed with air: Investigation of operational parameters. J Electroanal Chem 659:63–68. https://doi.org/10.1016/j.jelechem.2011.05.002

43. Khandegar V, K SAnil, (2014) Electrochemical treatment of textile effluent containing acid red 131 dye. J Hazard Toxic Radioact Waste 18:38–44. https://doi.org/10.1061/(ASCE)HZ.2153-5515.0000194

44. Daneshvar N, Khataee AR, Amani Ghadim AR, Rasoulifard MH (2007) Decolorization of C.I. Acid Yellow 23 solution by electrocoagulation process: Investigation of operational parameters and evaluation of specific electrical energy consumption (SEEC). J Hazard Mater 148:566–572. https://doi.org/10.1016/J.JHAZMAT.2007.03.028

45. Brillas E, Sirés I, Cabot PL (2010) Use of both anode and cathode reactions in wastewater treatment. In: Comninellis C, Chen G (eds) Electrochemistry for the environment. Springer, New York, pp 515–552

46. Yavuz Y, Öcal E, Koparal AS, Öğütveren ÜB (2011) Treatment of dairy industry wastewater by EC and EF processes using hybrid Fe● Al plate electrodes. J Chem Technol Biotechnol 86:964–969. https://doi.org/10.1002/jctb.2607

47. Varank G, Yazici Guvenc S, Demir A (2018) A comparative study of electrocoagulation and electro-Fenton for food industry wastewater treatment: Multiple response optimization and cost analysis. Sep Sci Technol 53:2727–2740. https://doi.org/10.1080/01496395.2018.1470643

48. Nayebi B, Ayati B (2021) Degradation of emerging amoxicillin compound from water using the electro-fenton process with an aluminum anode. Water Conserv Sci Eng. https://doi.org/10.1007/s41101-021-00101-4

49. Malakootian M, Moridi A (2017) Efficiency of electro-Fenton process in removing Acid Red 18 dye from aqueous solutions. Process Saf Environ Prot 111:138–147. https://doi.org/10.1016/j.psep.2017.06.008

50. Benitez FJ, Real FJ, Acero JL et al (2007) Kinetics of phenylurea herbicides oxidation by Fenton and photo-Fenton processes. J Chem Technol Biotechnol 82:65–73. https://doi.org/10.1002/jctb.1638

51. Yazdanbakhsh AR, Massoudinegad MR, Eliasi S, Mohammadi AS (2015) The influence of operational parameters on reduce of azithromyin COD from wastewater using the peroxi-electrocoagulation process. Journal of Water Process Engineering 6:51–57. https://doi.org/10.1016/j.jwpe.2015.03.005

52. Devika V, Gandhimathi R, Nidheesh PV, Ramesh ST (2016) Effect of solution pH on leachate treatment mechanism of peroxicoagulation process. J Hazard Toxic Radioact Waste 20:06016001. https://doi.org/10.1061/(ASCE)HZ.2153-5515.0000315

53. Kumar A, Nidheesh PV, Suresh Kumar M (2018) Composite wastewater treatment by aerated electrocoagulation and modified peroxi-coagulation processes. Chemosphere 205:587–593. https://doi.org/10.1016/J.CHEMOSPHERE.2018.04.141

54. Yıldıza N, Gökkuşa Ö, Koparalb AS, Yıldıza YŞ (2019) Peroxi-coagulation process: a comparison of the effect of oxygen level on color and TOC removals. Desalin Water Treat 1:9

55. Kishi A, Inoue M, Umeda M (2013) Evaluation of H2O2-generation during oxygen reduction at electrodeposited Pt particles on mask scratched electrodes. Appl Surf Sci 279:245–249. https://doi.org/10.1016/j.apsusc.2013.04.074

56. Guivarch E, Trevin S, Lahitte C, Oturan MA (2003) Degradation of azo dyes in water by Electro-Fenton process. Environ Chem Lett 1:38–44. https://doi.org/10.1007/s10311-002-0017-0

57. Nayir TY, Dinc O, Kara S et al (2020) Laundry wastewater treatment by peroxi-coagulation. Desalin Water Treat 182:98–108. https://doi.org/10.5004/dwt.2020.25188

58. Brillas E, Boye B, Dieng MM (2003) Peroxi-coagulation and photoperoxi-coagulation treatments of the herbicide 4-chlorophenoxyacetic acid in aqueous medium using an oxygen-diffusion cathode. J Electrochem Soc 150:E148. https://doi.org/10.1149/1.1543950

59. Sandhwar VK, Prasad B (2018) Comparison of electrocoagulation, peroxi-electrocoagulation and peroxi-coagulation processes for treatment of simulated purified terephthalic acid wastewater: optimization, sludge and kinetic analysis. Korean J Chem Eng 35:909–921. https://doi.org/10.1007/s11814-017-0336-2

Publisher's Note Springer Nature remains neutral with regard to jurisdictional claims in published maps and institutional affiliations.